

## Accepted Manuscript

Optimization of a binding fragment targeting the “enlarged methionine pocket” leads to potent *Trypanosoma brucei* methionyl-tRNA synthetase inhibitors

Wenlin Huang, Zhongsheng Zhang, Ranae M. Ranade, J. Robert Gillespie, Ximena Barros-Álvarez, Sharon A. Creason, Sayaka Shibata, Christophe L.M.J. Verlinde, Wim G.J. Hol, Frederick S. Buckner, Er kang Fan

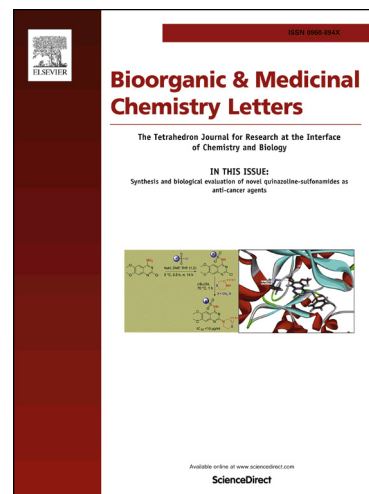
PII: S0960-894X(17)30424-9  
DOI: <http://dx.doi.org/10.1016/j.bmcl.2017.04.048>  
Reference: BMCL 24901

To appear in: *Bioorganic & Medicinal Chemistry Letters*

Received Date: 14 March 2017  
Accepted Date: 14 April 2017

Please cite this article as: Huang, W., Zhang, Z., Ranade, R.M., Robert Gillespie, J., Barros-Álvarez, X., Creason, S.A., Shibata, S., Verlinde, C.L.M., Hol, W.G.J., Buckner, F.S., Fan, E., Optimization of a binding fragment targeting the “enlarged methionine pocket” leads to potent *Trypanosoma brucei* methionyl-tRNA synthetase inhibitors, *Bioorganic & Medicinal Chemistry Letters* (2017), doi: <http://dx.doi.org/10.1016/j.bmcl.2017.04.048>

This is a PDF file of an unedited manuscript that has been accepted for publication. As a service to our customers we are providing this early version of the manuscript. The manuscript will undergo copyediting, typesetting, and review of the resulting proof before it is published in its final form. Please note that during the production process errors may be discovered which could affect the content, and all legal disclaimers that apply to the journal pertain.





## Optimization of a binding fragment targeting the “enlarged methionine pocket” leads to potent *Trypanosoma brucei* methionyl-tRNA synthetase inhibitors

Wenlin Huang,<sup>a</sup> Zhongsheng Zhang,<sup>a</sup> Ranae M. Ranade,<sup>b</sup> J. Robert Gillespie,<sup>b</sup> Ximena Barros-Álvarez,<sup>a,c</sup> Sharon A. Creason,<sup>b</sup> Sayaka Shibata,<sup>a</sup> Christophe L. M. J. Verlinde,<sup>a</sup> Wim G. J. Hol,<sup>a</sup> Frederick S. Buckner,<sup>b,\*</sup> Erkang Fan<sup>a,\*</sup>

<sup>a</sup> Department of Biochemistry, University of Washington, Seattle, WA 98195, United States

<sup>b</sup> Department of Medicine, Division of Allergy and Infectious Diseases, and the Center for Emerging and Re-emerging Infectious Diseases (CERID), University of Washington, Seattle, WA 98109, United States

<sup>c</sup> Laboratorio de Enzimología de Parásitos, Facultad de Ciencias, Universidad de los Andes, Mérida, Venezuela

### ARTICLE INFO

#### Article history:

Received  
Revised  
Accepted  
Available online

#### Keywords:

Human African trypanosomiasis  
Methionyl-tRNA synthetase  
Structure-based design  
*Trypanosoma brucei*

### ABSTRACT

Potent inhibitors of *Trypanosoma brucei* methionyl-tRNA synthetase were previously designed using a structure-guided approach. Compounds **1** and **2** were the most active compounds in the cyclic and linear linker series, respectively. To further improve cellular potency, SAR investigation of a binding fragment targeting the “enlarged methionine pocket” (EMP) was performed. The optimization led to the identification of a 6,8-dichloro-tetrahydroquinoline ring as a favorable fragment to bind the EMP. Replacement of 3,5-dichloro-benzyl group (the EMP binding fragment) of inhibitor **2** using this tetrahydroquinoline fragment resulted in compound **13**, that exhibited an EC<sub>50</sub> of 4 nM.

2009 Elsevier Ltd. All rights reserved.

Human African trypanosomiasis (HAT), commonly known as sleeping sickness, is a neglected tropical disease caused by the protozoan parasite *Trypanosoma brucei*.<sup>1</sup> The parasite is transmitted to humans through the bite of the tsetse fly. The disease progresses in two distinct stages: an initial acute stage where the parasitic infection is restricted to the hemolymphatic system and a late stage where the parasites cross the blood-brain barrier and reside in brain tissue.<sup>2</sup> Current treatment options are severely inadequate for this disease.<sup>1,3</sup> For the treatment of early stage infection, the two drugs, pentamidine and suramin, have toxicity and require injection.<sup>4</sup> The late stage infection is particularly difficult to treat, as drugs must cross the blood-brain barrier to be effective. The two drugs available for the late stage infection, melarsoprol and eflornithine, are toxic, have limited ability to cross the blood-brain barrier, and require injection.<sup>4,6</sup> New drugs that are safe and easy to administer are urgently needed for both stages of HAT.

We recently reported on structure-guided design of *Trypanosoma brucei* methionyl-tRNA synthetase (*TbMetRS*)

inhibitors.<sup>7</sup> Two series of compounds were designed and demonstrated to be potent *TbMetRS* inhibitors. The most potent compound in each series is shown in **Figure 1**. Compound **1** is a cyclic linker inhibitor with an EC<sub>50</sub> of 39 nM and compound **2** is a linear linker inhibitor with an EC<sub>50</sub> of 22 nM. In the previous study, the 3,5-dichlorophenyl moiety was fixed as the fragment to fill the so-called “enlarged methionine pocket” (EMP)<sup>8</sup> and the investigation was mainly focused on the linker part. Here, we report on the optimization of the EMP binding fragment based on the cyclic and linear linker compounds **1** and **2** in order to identify the preferred moiety for binding the EMP. This led to the identification of inhibitors with significantly enhanced potency.

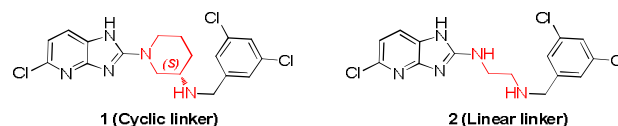
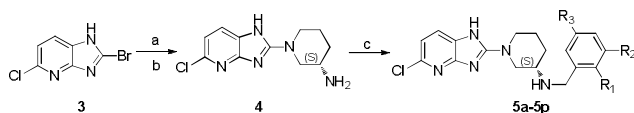


**Figure 1.** Structures of compounds **1** and **2**.

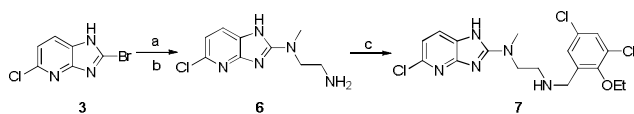
\* Corresponding authors

E-mail addresses: fbuckner@uw.edu (F.S. Buckner), erkang@uw.edu (E. Fan).

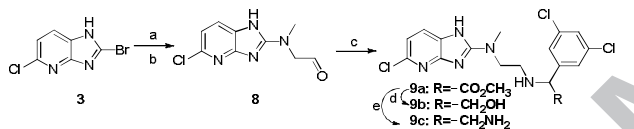
Analogues of compound **1** in which the 3,5-dichlorophenyl moiety was replaced by various 3,5-disubstituted phenyl or 2,3,5-trisubstituted phenyl ring were prepared as shown in **Scheme 1**. The synthesis was following previously reported procedures.<sup>7</sup> In brief, (*S*)-*tert*-butyl piperidin-3-ylcarbamate reacted with 2-bromo-5-chloro-3H-imidazo[4,5-*b*]pyridine through nucleophilic substitution reaction, and the following Boc removal provided intermediate **4**. Reductive amination of **4** with various substituted benzaldehydes afforded the final products **5a-5p**.



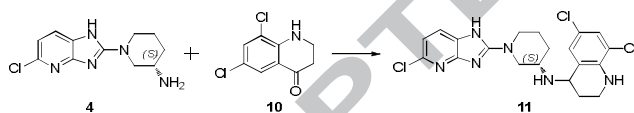
**Scheme 1.** Reagents and conditions: (a) (*S*)-*tert*-butyl piperidin-3-ylcarbamate, pyridine, MW, 100 °C, 30 min; (b) TFA, DCM, r.t. overnight; (c) Substituted benzaldehyde, DIPEA, NaBH<sub>3</sub>CN, AcOH, CH<sub>3</sub>OH, r.t., overnight.



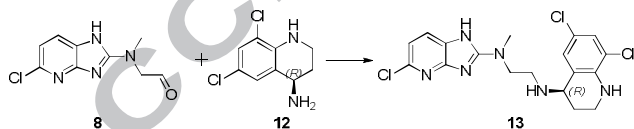
**Scheme 2.** Reagents and conditions: (a) *tert*-butyl (2-(methylamino)ethyl)carbamate, pyridine, MW, 100 °C, 30 min; (b) TFA, DCM, r.t. overnight; (c) 3,5-dichloro-2-ethoxybenzaldehyde, DIPEA, NaBH<sub>3</sub>CN, AcOH, CH<sub>3</sub>OH, r.t., overnight.



**Scheme 3.** Reagents and conditions: (a) 2,2-dimethoxy-*N*-methylethanamine, pyridine, MW, 100 °C, 60 min; (b) HCl (2 M), acetone, reflux, 60 min; (c) methyl 2-amino-2-(3,5-dichlorophenyl)acetate (HCl salt), DIPEA, NaBH<sub>3</sub>CN, AcOH, CH<sub>3</sub>OH, r.t., overnight; (d) LiAlH<sub>4</sub>, THF, 0 °C, 1h; (e) NH<sub>3</sub>, H<sub>2</sub>O, r.t. overnight.



**Scheme 4.** Reagents and conditions: Ti(OEt)<sub>4</sub>, EtOH, MW, 100 °C, 30 min; then NaBH<sub>3</sub>CN, MW, 100 °C, 8 h.



**Scheme 5.** Reagents and conditions: DIPEA, NaBH<sub>3</sub>CN, AcOH, CH<sub>3</sub>OH, r.t., overnight.

An analogue of compound **2** in which the 3,5-dichlorophenyl moiety was replaced by 3,5-dichloro-2-ethoxy phenyl was also designed, and synthesized as shown in **Scheme 2**. Compound **7** was synthesized following the same procedure used for synthesizing compound **5**. Additional analogues of compound **2** were prepared through introducing substituents onto the benzylic  $\alpha$ -position of the 3,5-dichlorophenyl ring (**Scheme 3**). Reagent 2,2-dimethoxy-*N*-methylethanamine reacted with 2-bromo-5-chloro-3H-imidazo[4,5-*b*]pyridine under the same microwave assisted nucleophilic substitution reaction, but with extended

reaction time. The resulted intermediate containing an acetal group was hydrolyzed under acidic condition to produce the aldehyde intermediate **8**, which underwent reductive amination with methyl 2-amino-2-(3,5-dichlorophenyl)acetate to generate compound **9a**. The methyl ester group of **9a** was reduced by lithium aluminum hydride to generate compound **9b**, while ammonolysis of the ester group produced compound **9c**.

Inspired by the superior potency of bacterial MetRS and *Tb*MetRS inhibitors that contained a tetrahydroquinoline group reported previously,<sup>9,11</sup> a 6,8-dichloro-tetrahydroquinoline group was employed to replace the 3,5-dichlorophenyl moiety in compounds **1** and **2** to generate compounds **11** and **13**. Their synthesis is shown in Schemes **4** and **5**. For compound **11**, amine and ketone were pre-reacted with Ti(OEt)<sub>4</sub> as catalyst, and the reductant NaBH<sub>3</sub>CN was added 30 min later followed by an 8 h reaction under microwave conditions (**Scheme 4**). Compound **13** was synthesized through reductive amination using intermediates **8** and **12** (**Scheme 5**). Intermediate **12** was prepared following previously published procedures.<sup>9</sup>

**Table 1.** Inhibitory activities of compounds against *Tb*MetRS enzyme and *T. brucei* cell growth

| Compound number       | R <sub>1</sub> /R <sub>2</sub> | Structure of R <sub>1</sub> /R <sub>2</sub> | IC <sub>50</sub> (nM) <sup>b</sup> | EC <sub>50</sub> (nM) <sup>c</sup> |
|-----------------------|--------------------------------|---|------------------------------------|------------------------------------|
| <b>1</b> <sup>a</sup> | R <sub>1</sub>                 |   | < 50                               | 39                                 |
| <b>2</b> <sup>a</sup> | R <sub>2</sub>                 |   | < 50                               | 22                                 |
| <b>5a</b>             | R <sub>1</sub>                 |   | < 50                               | 111                                |
| <b>5b</b>             | R <sub>1</sub>                 |   | < 50                               | 71                                 |
| <b>5c</b>             | R <sub>1</sub>                 |   | < 50                               | 85                                 |
| <b>5d</b>             | R <sub>1</sub>                 |   | < 50                               | 354                                |
| <b>5e</b>             | R <sub>1</sub>                 |   | < 50                               | 241                                |
| <b>5f</b>             | R <sub>1</sub>                 |   | < 50                               | 357                                |
| <b>5g</b>             | R <sub>1</sub>                 |   | < 50                               | 111                                |
| <b>5h</b>             | R <sub>1</sub>                 |   | < 50                               | 326                                |
| <b>5i</b>             | R <sub>1</sub>                 |   | < 50                               | 827                                |
| <b>5j</b>             | R <sub>1</sub>                 |   | < 50                               | 511                                |

|           |                |  |      |      |
|-----------|----------------|--|------|------|
| <b>5k</b> | R <sub>1</sub> |  | 389  | 3115 |
| <b>5l</b> | R <sub>1</sub> |  | 305  | 1703 |
| <b>5m</b> | R <sub>1</sub> |  | < 50 | 359  |
| <b>5n</b> | R <sub>1</sub> |  | < 50 | 230  |
| <b>5o</b> | R <sub>1</sub> |  | < 50 | 334  |
| <b>5p</b> | R <sub>1</sub> |  | < 50 | 40   |
| <b>7</b>  | R <sub>2</sub> |  | < 50 | 314  |
| <b>9a</b> | R <sub>2</sub> |  | 86   | 5273 |
| <b>9b</b> | R <sub>2</sub> |  | 101  | 995  |
| <b>9c</b> | R <sub>2</sub> |  | 75   | 4488 |
| <b>11</b> | R <sub>1</sub> |  | 89   | 57   |
| <b>13</b> | R <sub>2</sub> |  | < 50 | 4    |

<sup>a</sup>Data was published previously, included here for comparison; <sup>b</sup>The values are averages of triplicate data, control for *TbMetRS* IC<sub>50</sub> assay: Met-SA1<sup>7</sup> (± 10.1%; n = 11 assays); <sup>c</sup>The values are averages of triplicate data, control for *TbEC*<sub>50</sub> assay: Pentamidine (± 15.5%; n=9).

All the compounds were first evaluated for enzymatic potency against *TbMetRS* using an ATP depletion assay as described previously.<sup>7,12</sup> As shown in **Table 1**, most of the compounds are very potent inhibitors of *TbMetRS*, exhibiting IC<sub>50</sub>s below 50 nM (the enzyme concentration used in the assay). Compounds **5k** and **5l** were found to have significantly reduced inhibitory potency compared to **1**, with IC<sub>50</sub>s >300 nM.

All the compounds were also tested for potency against *T. brucei* parasites using a growth inhibition assay as previously described.<sup>7,9,13</sup> The results are shown in Table 1 and the inhibition curves of compounds with EC<sub>50</sub> < 100 nM are shown in Figure S1 (Supporting Information). Compounds with larger groups at the 3- and 5-positions, such as bromo and cyano (**5a-5c**), were tolerated by the enzyme, but had higher EC<sub>50</sub> values by 2-3 folds. All compounds that contain the 2,3,5-trisubstituted phenyl ring except **5p** were less potent in the parasite growth inhibition assay. The ethoxy group was the best 2-position substituent as evidenced by **5g** and **5p** being more potent than their counterparts with other substituents. In fact the cellular potency of compound **5p** was nearly identical to the EC<sub>50</sub> of **1** (39 nM). Larger alkoxy groups at 2-position resulted in significant reductions in cellular activity, especially for branched alkoxy groups. In general, the larger the alkoxy group at the 2-position, the less cellular potency the compound exhibited (**5g**<**5h**<**5j**<**5i**). Compounds **5k** and **5l**

that contain branched alkoxy groups at 2-position lost cellular potency significantly. Compounds **9a-9c** that contain substitutions at the benzylic  $\alpha$ -position in the case of the linear linker series exhibited weak cellular potency. The 6,8-dichloro-tetrahydroquinoline moiety was a good match for the linear linker series, but not in the cyclic linker series as indicated by compounds **11** and **13**. In the cyclic linker series, compound **11** was less potent than **1**, while in the linear linker series, compound **13** was more potent than **2**. Compound **13** was the most potent compound found in this study, exhibiting an EC<sub>50</sub> of 4 nM. The calculated physicochemical properties of compounds with EC<sub>50</sub> <100 nM against *T. brucei* are presented in Table S1 (Supporting Information). All these potent compounds possess Ligand Efficiency (LE) values > 0.3, indicating a good balance of size and lipophilicity. It is noteworthy that compounds **2** and **13** show the highest LE of 0.43, and the Ligand-Lipophilicity Efficiency (LLE) of 2.96 and 4.38, respectively. This indicates the optimization of **2** to **13** not only improved potency but also maintained LE and increased LLE.

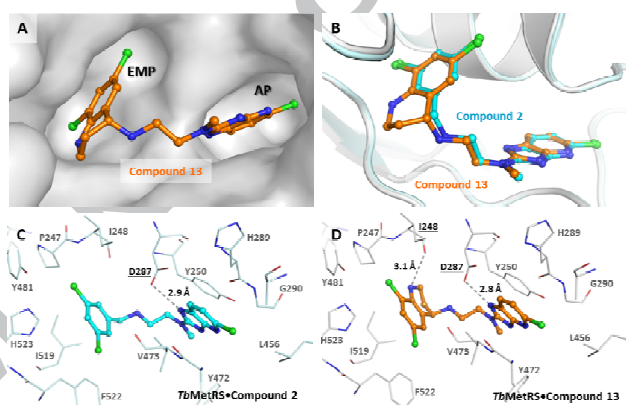


**Figure 2.** Binding of compound **13** to *TbMetRS*. (A) *TbMetRS*•Compound **13** complex structure (PDB: 5V49). The protein surface and the two pockets, EMP and AP, where the inhibitor is bound are shown. Protein carbon atoms are colored grey, nitrogens blue and oxygens red. (B) Superposition of *TbMetRS* structures bound to compounds **13** and **2** (PDB: 5I59).<sup>7</sup> Chlorine atoms are colored green, carbon atoms of compounds **13** and **2** are colored orange and cyan, respectively. (C and D) Hydrogen bond interactions in *TbMetRS*•compound **2** and *TbMetRS*•compound **13** structures are shown with dotted lines and labels for interacting residues are underlined.

To check for unexpected changes in the binding mode, we obtained crystal structure of *TbMetRS* in complex with compounds **13** at 2.3Å resolution (Figure 2A). The binding mode of compound **13** was compared to compound **2** bound to *TbMetRS* (Figure 2B). The 5-chloro-imidazopyridine group of compound **13** bound in the same manner to the auxiliary pocket (AP) as the corresponding part in compound **2**, forming a hydrogen bond interaction with the catalytic residue Asp287 (Figures 2C, 2D). The linkers of both compounds superimposed almost perfectly (Figure 2B). The 6,8-dichloro-tetrahydroquinoline ring of compound **13** also bound similarly to the EMP compared to the 3,5-dichloro-benzyl group in compound **2**, as observed before for analogs with longer linkers.<sup>9</sup> The dichloro benzene group of compound **2** was in essentially the same position as the corresponding part in compound **13**. The availability of compound **13** bound crystal structure could help to explain the structure-activity relationship (SAR) data generated in **Table 1** and guide future inhibitor design.

Potent compounds with EC<sub>50</sub> <100 nM against *T. brucei* were selected to examine the host cell toxicity. The compounds shown in **Table 2** were tested using a human lymphoblast cell line (CRL-8155) and a hepatocellular carcinoma cell line (Hep G2)

following procedures described previously.<sup>7,14</sup> Compounds **5b** and **5c** had CC<sub>50</sub>s (concentration to cause 50% cytotoxicity) close to or greater than 40 μM, whereas compounds **11** and **13** had CC<sub>50</sub>s of ~20 μM, and compound **5p** had CC<sub>50</sub> of ~10 μM. Overall, these compounds exhibited low toxicities to mammalian cell lines.

Compounds with good cellular potency were further tested for oral pharmacokinetic (PK) properties and/or brain penetration in mice (**Table 2**). The PK studies were performed following published procedures with compounds being administered by oral gavage at 50 mg/kg.<sup>7,9,15-17</sup> The brain permeability was tested at a dose of 5 mg/kg IP as described previously.<sup>7,9</sup> Compound **5b** exhibited high plasma exposure comparable to compound **1** with a C<sub>max</sub> at 19.2 μM, and an AUC of 4687.5 min·μM. Unfortunately, like compound **1**, the brain permeability of **5b** was poor with undetectable brain levels at 60 min after IP injection. Compound **5p**, the 2,3,5-trisubstituted analogue of **1**, showed slightly improved brain/ plasma ratio but less favorable oral PK compared to **1**. Compound **11** had promising PK properties with a C<sub>max</sub> at 14.7 μM and AUC of 947.4 min·μM, whereas compound **13** showed low plasma exposure. Both the plasma and brain exposure of **13** are lower than those of **2**, but its improvement in EC<sub>50</sub> over **2** may compensate for the lower exposure in an in vivo efficacy model.

**Table 2.** Toxicity, oral PK, and brain penetration data of select compounds.

| Cpd.                  | CRL-8155<br>(μM) <sup>b</sup> | Hep G2<br>(μM) <sup>c</sup> | Oral PK (50 mg/kg) <sup>d</sup> |                          | Brain/Plasma<br>Ratio (%) <sup>d</sup> |
|-----------------------|-------------------------------|-----------------------------|---------------------------------|--------------------------|--|
|                       |                               |                             | AUC<br>(min·μM)                 | C <sub>max</sub><br>(μM) |  |
| <b>1</b> <sup>a</sup> | 29.3                          | 49.0                        | 6223±2160                       | 37.6±22.1                | 0                                      |
| <b>2</b> <sup>a</sup> | 22.6                          | 39.2                        | 952±331                         | 9.7±4.5                  | 27.2±7.1                               |
| <b>5b</b>             | 43.0                          | >50                         | 4688±2123                       | 19.2±16.4                | 0                                      |
| <b>5c</b>             | 47.6                          | 39.1                        | Not done                        | Not done                 | Not done                               |
| <b>5p</b>             | 10.5                          | 18.7                        | 182±43                          | 2.1±1.5                  | 4.4±0.6                                |
| <b>11</b>             | 19.0                          | 40.2                        | 947±354                         | 14.7±4.3                 | Not done                               |
| <b>13</b>             | 18.5                          | 30.6                        | 140±40                          | 1.3±0.7                  | 19.1±7.5                               |

<sup>a</sup>Data was published previously, included here for comparison; <sup>b</sup>The values are averages of quadruplicate, control for CRL-8155 EC<sub>50</sub> assay: Quinacrine (± 12.5%; n=2); <sup>c</sup>The values are averages of quadruplicate, control for HepG2 EC<sub>50</sub> assay: Quinacrine (± 14.9%; n=3); <sup>d</sup>The values are from one experiment with 3 mice per group.

In summary, a series of 3,5-disubstituted and 2,3,5-trisubstituted benzyl groups, as well as a 6,8-dichloro-tetrahydroquinoline moiety were used to replace the 3,5-dichlorobenzyl group as the EMP binding moiety based on previously discovered cyclic and linear linker *TbMetRS* inhibitors. It was found that substituents larger than chloro at 3- and/or 5-positions do not improve potency while 2,3,5-trisubstituted benzyl groups generally resulted in decreased potency. Substituents at the benzylic  $\alpha$ -position in the case of the linear linker series also led to a loss of potency. The 6,8-dichloro-tetrahydroquinoline moiety however, afforded compound **13** in the linear linker series with improved potency against *T. brucei* parasites. We obtained the crystal structure of *TbMetRS* in complex with compound **13** which will help guide future inhibitor design. Compound **13** also had moderately good brain penetration in mice. This study identified potentially better fragments for binding the EMP than the 3,5-dichloro benzyl group in the cyclic and linear linker series of *TbMetRS* inhibitors.

## Acknowledgments

Research reported in this publication was supported by the National Institute of Allergy and Infectious Diseases of the National Institutes of Health under award numbers R01AI084004 and R01AI097177. We acknowledge the support of a Fulbright Fellowship to X.B.-A. We thank Stewart Turley and Robert Steinfeldt for providing support for the X-ray data collection and computing environment at the Biomolecular Structure Center of the University of Washington. Crystallography performed in support of the work benefitted from remote access to resources at the Stanford Synchrotron Radiation Lightsource supported by the U.S. Department of Energy Office of Basic Energy Sciences under Contract No. DE-AC02-76SF00515 and by the National Institutes of Health (P41GM103393).

## References

- Brun, R.; Blum, J.; Chappuis, F.; Burri, C., Human African trypanosomiasis. *Lancet* 375, **2010**, 148.
- Grab, D. J.; Kennedy, P. G. E., Traversal of human and animal trypanosomes across the blood-brain barrier. *Journal of Neurovirology* **2008**, 14, 344.
- Rodgers, J., Human African trypanosomiasis, chemotherapy and CNS disease. *J. Neuroimmunol.* **2009**, 211, 16.
- Trypanosomiasis, human African (sleeping sickness). <http://www.who.int/mediacentre/factsheets/fs259/en/>, **2016** (accessed 12.06.16).
- Croft, S. L.; Barrett, M. P.; Urbina, J. A., Chemotherapy of trypanosomiasis and leishmaniasis. *Trends. Parasitol.* **2005**, 21, 508.
- Wilkinson, S. R.; Kelly, J. M., Trypanocidal drugs: mechanisms, resistance and new targets. *Expert. Rev. Mol. Med.* **2009**, 11.
- Huang, W.; Zhang, Z.; Barros-Álvarez, X.; Koh, C. Y.; Ranade, R. M.; Gillespie, J. R.; Creason, S. A.; Shibata, S.; Verlinde, C. L. M.; Hol, W. G. J.; Buckner, F. S.; Fan, E., Structure-guided design of novel *Trypanosoma brucei* Methionyl-tRNA synthetase inhibitors. *Eur. J. Med. Chem.* **2016**, 124, 1081.
- Koh, C. Y.; Kim, J. E.; Shibata, S.; Ranade, R. M.; Yu, M.; Liu, J.; Gillespie, J. A. R.; Buckner, F. S.; Verlinde, C. L. M. J.; Fan, E.; Hol, W. G. J., Distinct States of Methionyl-tRNA Synthetase Indicate Inhibitor Binding by Conformational Selection. *Structure.* **2012**, 20, 1681.
- Zhang, Z.; Koh, C. Y.; Ranade, R. M.; Shibata, S.; Gillespie, J. R.; Hulverson, M. A.; Huang, W.; Nguyen, J.; Pendem, N.; Gelb, M. H.; Verlinde, C. L. M. J.; Hol, W. G. J.; Buckner, F. S.; Fan, E., 5-Fluoroimidazo[4,5-b]pyridine Is a privileged fragment that conveys bioavailability to potent Trypanosomal methionyl-tRNA synthetase inhibitors. *ACS Infect. Dis.* **2016**, 2, 399.
- Jarvest, R. L.; Berge, J. M.; Berry, V.; Boyd, H. F.; Brown, M. J.; Elder, J. S.; Forrest, A. K.; Fosberry, A. P.; Gentry, D. R.; Hibbs, M. J.; Jaworski, D. D.; O'Hanlon, P. J.; Pope, A. J.; Rittenhouse, S.; Sheppard, R. J.; Slater-Radosti, C.; Worby, A., Nanomolar inhibitors of *Staphylococcus aureus* methionyl tRNA synthetase with potent antibacterial activity against Gram-positive pathogens. *J. Med. Chem.* **2002**, 45, 1959.
- Jarvest, R. L.; Armstrong, S. A.; Berge, J. M.; Brown, P.; Elder, J. S.; Brown, M. J.; Copley, R. C. B.; Forrest, A. K.; Hamprecht, D. W.; O'Hanlon, P. J.; Mitchell, D. J.; Rittenhouse, S.; Witty, D. R., Definition of the heterocyclic pharmacophore of bacterial methionyl tRNA synthetase inhibitors: potent antibacterially active non-quinolone analogues. *Bioorg. Med. Chem. Lett.* **2004**, 14, 3937.
- Pedro-Rosa, L.; Buckner, F. S.; Ranade, R. M.; Eberhart, C., Madoux, F.; Gillespie, J. R.; Koh, C. Y.; Brown, S.; Lohse, J.; Verlinde, C. L. M., Fan, E., Bannister, T., Scampavia, L., Hol, W. G. J., Spicer, T., and Hodder, P. Identification of potent inhibitors of the *Trypanosoma brucei* methionyl-tRNA synthetase via high throughput orthogonal screening. *J. Biomol. Screening.* **2015**, 20, 122.
- Shibata, S.; Gillespie, J. R.; Kelley, A. M.; Napuli, A. J.; Zhang, Z.; Kovzun, K. V.; Pefley, R. M.; Lam, J.; Zucker, F. H.; Van Voorhis, W. C.; Merritt, E. A.; Hol, W. G.; Verlinde, C. L.; Fan, E.; Buckner, F. S., Selective inhibitors of methionyl-tRNA

- synthetase have potent activity against *Trypanosoma brucei* infection in mice. *Antimicrob. Agents. Chemother.* **2011**, 55, 1982.
14. Shibata, S.; Gillespie, J. R.; Ranade, R. M.; Koh, C. Y.; Kim, J. E.; Laydbak, J. U.; Zucker, F. H.; Hol, W. G.; Verlinde, C. L.; Buckner, F. S.; Fan, E., Urea-based inhibitors of *Trypanosoma brucei* Methionyl-tRNA synthetase: selectivity and in vivo characterization. *J. Med. Chem.* **2012**, 55, 6342.
  15. Kraus, J. M.; Verlinde, C. L. M. J.; Karimi, M.; Lepesheva, G. I.; Gelb, M. H.; Buckner, F. S., Rational modification of a candidate cancer drug for use against Chagas disease. *J. Med. Chem.* **2009**, 52, 1639–1647.
  16. Suryadevara, P. K.; Olepu, S.; Lockman, J. W.; Ohkanda, J.; Karimi, M.; Verlinde, C. L. M. J.; Kraus, J. M.; Schoepe, J.; Van Voorhis, W. C.; Hamilton, A. D.; Buckner, F. S.; Gelb, M. H., Structurally simple inhibitors of Lanosterol 14 $\alpha$ -demethylase are efficacious in a rodent model of acute Chagas disease. *J. Med. Chem.* **2009**, 52, 3703.
  17. Tatipaka, H. B.; Gillespie, J. R.; Chatterjee, A. K.; Norcross, N. R.; Hulverson, M. A.; Ranade, R. M.; Nagendar, P.; Creason, S. A.; McQueen, J.; Duster, N. A.; Nagle, A.; Supek, F.; Molteni, V.; Wenzler, T.; Brun, R.; Glynne, R.; Buckner, F. S.; Gelb, M. H., Substituted 2- phenylimidazopyridines: A new class of drug leads for human African Trypanosomiasis. *J. Med. Chem.* **2014**, 57, 828.

## Graphical Abstract

Optimization of a binding fragment targeting the “enlarged methionine pocket” leads to potent *Trypanosoma brucei* methionyl-tRNA synthetase inhibitors

Leave this area blank for abstract info.

Wenlin Huang, Zhongsheng Zhang, Ranae M. Ranade, J. Robert Gillespie, Ximena Barros-Álvarez, Sharon A. Creason, Sayaka Shibata, Christophe L. M. J. Verlinde, Wim G. J. Hol, Frederick S. Buckner, Erkang Fan

